LETTER

doi:10.1038/nature09584

# mTORC1 controls fasting-induced ketogenesis and its modulation by ageing

Shomit Sengupta[1,2,3], Timothy R. Peterson[1,2,3], Mathieu Laplante[1,2,3], Stephanie Oh[1,2,3] & David M. Sabatini[1,2,3]

**The multi-component mechanistic target of rapamycin complex 1 (mTORC1) kinase is the central node of a mammalian pathway that coordinates cell growth with the availability of nutrients, energy and growth factors[1]. Progress has been made in the identification of mTORC1 pathway components and in understanding their functions in cells, but there is relatively little known about the role of the pathway *in vivo*. Specifically, we have little knowledge regarding the role mTOCR1 has in liver physiology. In fasted animals, the liver performs numerous functions that maintain whole-body homeostasis, including the production of ketone bodies for peripheral tissues to use as energy sources. Here we show that mTORC1 controls ketogenesis in mice in response to fasting. We find that liver-specific loss of TSC1 (tuberous sclerosis 1), an mTORC1 inhibitor[1], leads to a fasting-resistant increase in liver size, and to a pronounced defect in ketone body production and ketogenic gene expression on fasting. The loss of raptor (regulatory associated protein of mTOR, complex 1) an essential mTORC1 component[1], has the opposite effects. In addition, we find that the inhibition of mTORC1 is required for the fasting-induced activation of PPARα (peroxisome proliferator activated receptor α), the master transcriptional activator of ketogenic genes[2], and that suppression of NCoR1 (nuclear receptor co-repressor 1), a co-repressor of PPARα[3], reactivates ketogenesis in cells and livers with hyperactive mTORC1 signalling. Like livers with activated mTORC1, livers from aged mice have a defect in ketogenesis[4,5], which correlates with an increase in mTORC1 signalling. Moreover, we show that the suppressive effects of mTORC1 activation and ageing on PPARα activity and ketone production are not additive, and that mTORC1 inhibition is sufficient to prevent the ageing-induced defect in ketogenesis. Thus, our findings reveal that mTORC1 is a key regulator of PPARα function and hepatic ketogenesis and suggest a role for mTORC1 activity in promoting the ageing of the liver.**

Whereas mice lacking the mTORC1 components mTOR or raptor die in early embryogenesis[6], mice treated with pharmacological inhibitors of mTORC1 or with tissue-specific deletions of raptor or mTOR are viable, and are beginning to reveal diverse roles for mTORC1 in adult physiology[6]. To begin the study of mTORC1 in liver physiology, we determined the effects of fasting and feeding on hepatic mTORC1 activity. In fasted mice, mTORC1 activity in the liver was low (Fig. 1a, Supplementary Fig. 1a), as detected by the phosphorylation of the ribosomal S6 protein, an established marker of mTORC1 pathway activity. Refeeding led to an increase in phospho-S6 levels that was blocked by rapamycin, an mTORC1 inhibitor. mTORC1 activation preceded that of Akt (Fig. 1b), an effector of the insulin-activated PI3K pathway, which is consistent with mTORC1 responding not only to insulin but also to other food-triggered signals, such as nutrients.

We examined the functions of mTORC1 in the liver using genetically engineered mice with the liver-specific deletion of the gene for raptor, or TSC1, a negative regulator of mTORC1 (Fig. 1c) (Methods). We refer to mice lacking hepatic TSC1 or raptor as Li-*Tsc1*$^{KO}$ or Li-*Rap*$^{KO}$ mice, respectively. In Li-*Tsc1*$^{KO}$ mice, the mTORC1 pathway was constitutively active and not affected by fasting or feeding, while the loss of raptor eliminated mTORC1 activity irrespective of feeding status (Fig. 1d). Compared to controls, TSC1 or raptor deletion led to an ~40% increase or decrease, respectively, in liver mass, hepatocyte size, and protein content (Fig. 1e; Supplementary Fig. 1b, c). Whereas in control animals a 24-h fast caused a ~25% reduction in liver mass, the livers of Li-*Tsc1*$^{KO}$ mice were largely refractory to the shrinking effects of fasting. In addition, fasting did not further decrease the size of the already small livers of Li-*Rap*$^{KO}$ mice (Fig. 1e). Thus, mTORC1 is strongly regulated by fasting and feeding and plays a major role in setting liver size in response to the nutritional state.

We measured the levels of several serum and liver metabolites in control, Li-*Tsc1*$^{KO}$ and Li-*Rap*$^{KO}$ mice that were fasted or given *ad libitum* access to food (Supplementary Fig. 1d). Because mTORC1 activation suppresses Akt signalling[7] (Supplementary Fig. 1e), we also examined Li-*Ir*$^{KO}$ (also known as LIRKO; ref. 8) mice that lack the Insulin Receptor in the liver and thus have attenuated Akt signalling[8]. Levels of most serum and hepatic metabolites were not significantly affected by TSC1 loss, except that fasted Li-*Tsc1*$^{KO}$ mice had markedly low serum ketones, a phenotype not shared by Li-*Ir*$^{KO}$ mice (Fig. 2a; Supplementary Fig. 1d, f, g). Compared to control animals, Li-*Tsc1*$^{KO}$ mice had decreased locomotor activity and body temperature upon fasting (Supplementary Fig. 1h, i), phenotypes also observed in other mutant mice with defective ketogenesis[9].

The ketone bodies, acetoacetate and β-hydroxybutyrate, are produced by the liver primarily from fatty acids released by adipose tissue and are used by tissues to generate acetyl-CoA for energy production during fasting. The defect in ketone production in Li-*Tsc1*$^{KO}$ mice is not due to an impairment in fatty acid uptake by the liver, as they were unable to generate ketones even when given sodium octanoate, a fatty acid that freely diffuses into liver mitochondria and serves as a ketogenic substrate[10] (Supplementary Fig. 2a).

As Li-*Tsc1*$^{KO}$ mice have a defect in ketone production when fasted, we asked if Li-*Rap*$^{KO}$ mice could produce ketones when fed. Li-*Rap*$^{KO}$ mice given food *ad libitum* do not have elevated levels of ketones (Fig. 2a), perhaps because the serum fatty acids that are ketogenic substrates are at low levels in fed mice[11]. Indeed, when Li-*Rap*$^{KO}$ mice were administered the ketogenic substrate sodium octanoate upon refeeding after a fast, they did produce ketones for several hours after feeding, even at times when ketone levels had dropped precipitously in control animals (Supplementary Fig. 2b). Furthermore, Li-*Rap*$^{KO}$ or rapamycin-treated mice do have elevated serum ketones at the short times after refeeding when the control animals already have baseline ketone levels (Supplementary Fig. 2c, d).

The defect in ketogenesis in the Li-*Tsc1*$^{KO}$ mice is liver-autonomous, as liver tissue from these mice failed to oxidize fatty acids or produce ketones *ex vivo* (Fig. 2b). To confirm these results in cells *in vitro*, we developed a ketogenic media containing the PPARα agonist WY-14643 (Methods) that induces ketone production in murine AML12 hepatocytes (Fig. 2c). Consistent with the *in vivo* and *ex vivo* findings, the suppression of TSC1 or TSC2 inhibited, in a rapamycin-sensitive

[1]Whitehead Institute for Biomedical Research, Nine Cambridge Center, Cambridge, Massachusetts 02142, USA. [2]Howard Hughes Medical Institute, Department of Biology, Massachusetts Institute of Technology, Cambridge, Massachusetts 02139, USA. [3]The David H. Koch Institute for Integrative Cancer Research at MIT, 77 Massachusetts Avenue, Cambridge, Massachusetts 02139, USA.

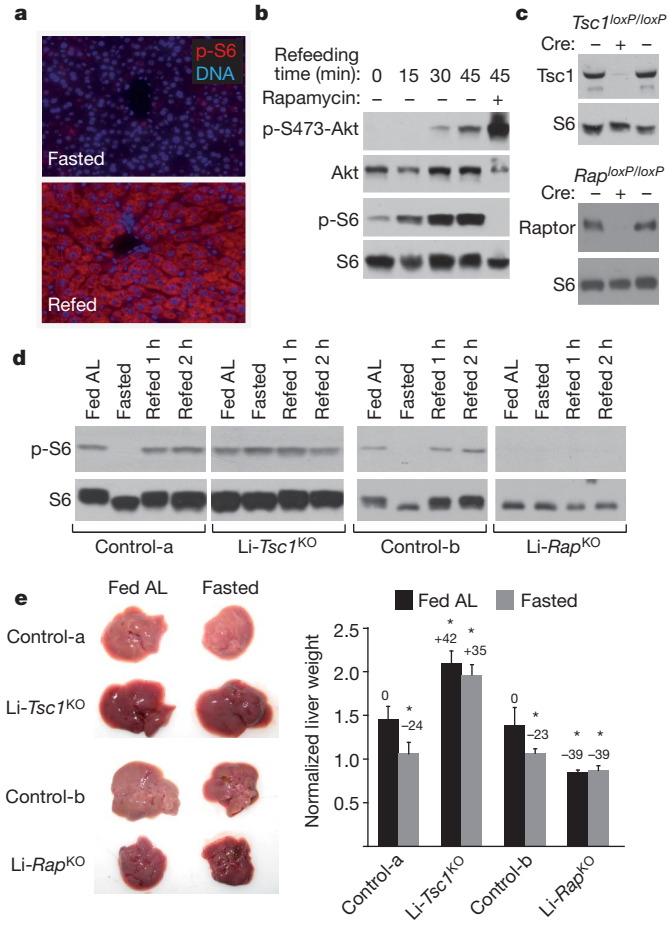


**Figure 1 | In the liver, mTORC1 activity is sensitive to fasting and feeding and regulates organ size.** **a**, Images of liver sections from mice fasted for 24 h or fasted and refed for 45 min, and co-stained for serine 240/244 phosphorylated-S6 (p-S6; red) and DNA (blue). **b**, Mice were fasted for 24 h or fasted and then refed for 15, 30 or 45 min, or injected with rapamycin 2 h before refeeding for 45 min. Liver lysates were analysed by immunoblotting for the indicated proteins and phosphorylation states. **c**, Immunoblot analyses for TSC1 or raptor protein in liver lysates from indicated mouse strains that have or do not have Cre recombinase expression in the liver. **d**, Indicated mice were killed after being given food *ad libitum* (fed AL), fasted for 24 h (fasted), or fasted and refed for 1 or 2 h. Liver lysates were analysed by immunoblotting for the levels of S6 and serine 240/244 phosphorylated-S6. Control-a are $Tsc1^{loxP/loxP}$ mice administered the empty adenovirus, and control-b are $Rap^{loxP/loxP}$ mice not carrying the Albumin-Cre transgene. The same nomenclature is used in the subsequent figures. **e**, Gross images of livers from Li-$Tsc1^{KO}$ or Li-$Rap^{KO}$ mice that were fed *ad libitum* or fasted for 24 h (fasted). Bar graph shows mean ± s.d. normalized liver weight for $n \geq 5$. The percentage changes in liver weight compared to respective fed control mice are indicated. $^*P < 0.05$ compared to respective fed control mice.

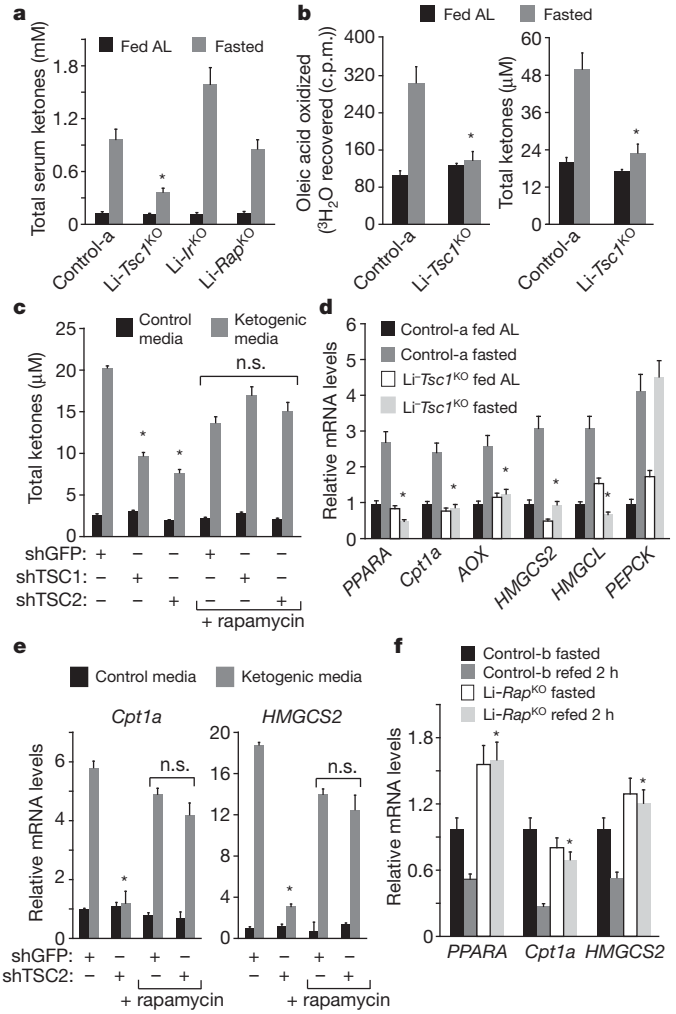


**Figure 2 | mTORC1 inhibits ketogenesis and PPARα activity in a liver autonomous fashion.** **a**, Fed mice were given *ad libitum* access to food and killed at the beginning of the day. Fasted mice were denied food for 24 h and killed at the same time of day as the fed mice. Indicated values are mean ± s.d. for $n \geq 6$; $^*P < 0.05$ compared to fasted control mice. **b**, Indicated measurements were made as described in Methods using liver tissue isolated from control or Li-$Tsc1^{KO}$ mice that had *ad libitum* access to food (fed) or had been fasted for 24 h. Values are mean ± s.d. for $n = 4$. $^*P < 0.05$ compared to fasted control mice. **c**, AML12 cells stably expressing validated lentiviral shRNAs targeting GFP, TSC1 or TSC2 were placed in control or ketogenic media with or without 20 nM rapamycin. Total ketones in the culture media were determined after a 3-day incubation. Values are mean ± s.d. for $n = 6$. $^*P < 0.05$ compared to shGFP-expressing cells cultured in ketogenic media. n.s., no significant differences between bracketed values. **d**, mRNA levels were quantified by qRT–PCR in total RNA isolated from indicated liver samples. Values are mean ± s.d. for $n \geq 8$. $^*P < 0.05$ compared to fasted control mice. **e**, mTORC1 activation inhibits, in a rapamycin-sensitive fashion, PPARα-target gene expression in cells in culture. mRNA levels were determined as in **d** from the AML12 cells used in **c**. Values are mean ± s.d. for $n = 6$. $^*P < 0.05$ compared to shGFP-expressing cells growing in ketogenic media. **f**, Control and Li-$Rap^{KO}$ mice were fasted for 24 h and then refed for 2 h. Levels of indicated mRNAs were measured as in **d**. Values are mean ± s.d. for $n \geq 4$. $^*P < 0.05$ compared to refed control mice.

fashion, ketone production by AML12 cells (Fig. 2c; Supplementary Fig. 3a). Taken together, our loss of function data indicate that mTORC1, in a liver-autonomous fashion, is a key regulator of ketone production in response to fasting.

Because the nuclear hormone receptor PPARα is a master activator of the hepatic ketogenic gene expression program in response to fasting[2], we asked if mTORC1 controls ketogenesis by modulating PPARα function. PPARα transactivates its own gene as well as those for enzymes required for fatty acid oxidation and ketogenesis, such as Cpt1a, AOX, HMGCS2 and HMGCL[12]. Fasting increased the mRNA levels of PPARα and its target genes in control, but not TSC1-null, livers (Fig. 2d). In contrast, loss of TSC1 did not block the fasting-induced increase in the mRNA for PEPCK, which is not a target of PPARα (Fig. 2d). In Li-$Tsc1^{KO}$ mice, WY-14643, the synthetic PPARα agonist[3], did not increase serum ketones or PPARα-target gene expression in the liver (Supplementary Fig. 2e, f), but did activate PPARα in the small intestine (a secondary site of ketogenesis), confirming that Li-$Tsc1^{KO}$ mice have liver-specific defects in PPARα function (Supplementary Fig. 2f). In accord with the *in vivo* findings, a knockdown of TSC2 in AML12 cells inhibited PPARα in a rapamycin-sensitive fashion (Fig. 2e). Lastly, as suggested by the capacity of Li-$Rap^{KO}$ mice to produce ketones in the fed state (Supplementary

Fig. 2b), feeding did not downregulate the expression of PPARα and its target genes in the livers of Li-*Rap*$^{KO}$ mice (Fig. 2f) or in mice treated with rapamycin before feeding (Supplementary Fig. 2g). Because PPARα overexpression did not restore PPARα-target gene expression in livers or AML12 cells with activated mTORC1 (Supplementary Fig. 4a–f), these results are consistent with mTORC1 negatively regulating ketogenesis by preventing the activation of PPARα. Unlike mice lacking PPARα[13], those without TSC1 do not have hepatic steatosis upon fasting, perhaps because plasma triglyceride and hepatic microsomal triglyceride transfer protein (MTTP) levels are increased in these mice (Supplementary Fig. 1d and data not shown), suggesting that mTORC1 promotes very low density lipoprotein assembly and secretion.

In the fed state, PPARα interacts with the NCoR1 and SMRT corepressors, which suppress ketogenic gene expression by recruiting histone deacetylases[14]. Upon fasting, ligand-binding to PPARα initiates corepressor release and the association of coactivators, like p300 or CBP, which activate ketogenic genes by recruiting histone acetylases[15]. In the livers of control animals, fasting led to an increase in histone acetylation at PPARα response element (PPRE)-containing promoters, which correlated with the loss and gain of NCoR1 and p300, respectively, from the promoters (Fig. 3a–c). In contrast, in TSC1-null livers, NCoR1 did not exit the PPRE-containing promoters upon fasting, and p300 occupancy and histone acetylation remained in a fed-like state (Figs 3a–c). Raptor-null livers had the opposite phenotypes (Supplementary Fig. 5a, b) and TSC1 loss did not affect the binding of PPARα to promoters (Supplementary Fig. 5c). In AML12 cells, the knockdown of TSC2 repressed the disassociation of NCoR1 from PPRE-containing promoters, even when the cells were treated with the PPARα ligand (Supplementary Fig. 5d). The suppression of NCoR1 restored ketone production and PPARα-target gene expression in TSC2-deficient AML12 cells and livers (Fig. 3d, e, Supplementary Fig. 6a–c), while the histone deacetylase inhibitor trichostatin A reversed the defect in ketone production in AML12 cells caused by mTORC1 activation (Supplementary Fig. 6d).

As these results suggested an active role for NCoR1 in the inhibition of ketogenesis and PPARα by mTORC1, we asked if mTORC1 regulates NCoR1 function. Because mTORC1 did not affect NCoR1 protein levels (data not shown), we considered the possibility that fasting and feeding control the nuclear localization of NCoR1 in an mTORC1-dependent fashion. Quantitative imaging assays using an antibody that recognizes endogenous NCoR1 (Supplementary Fig. 7a) showed that NCoR1 was present in both the cytoplasm and nuclei of hepatocytes in fed animals but only in the cytoplasm in fasted mice (Supplementary Fig. 8a). The loss of TSC1 led to the presence of NCoR1 in the nucleus even in fasted mice (Supplementary Fig. 8a), while that of raptor prevented the feeding-induced movement of NCoR1 into the nucleus (Supplementary Fig. 8b). Analogous results were obtained with endogenous or epitope-tagged recombinant NCoR1 in cultured AML12 cells (Supplementary Figs 7b, 8c). Thus, mTORC1 regulates the subcellular localization of NCoR1, providing a potential mechanism for how mTORC1 might control PPARα and ketogenesis.

Given that mTORC1 regulates ketogenesis and previous work showing that ageing blunts PPARα-target gene expression and ketone production in rodents[4,5], we asked if mTORC1 mediates the effects of ageing on ketogenesis. If this were the case, the inhibitory effects on ketogenesis of mTORC1 activation and ageing should not be additive. Indeed, while the loss of TSC1 in young mice reduced serum ketones and hepatic PPARα-target gene expression, the deletion of TSC1 in aged mice (Supplementary Fig. 3c) did not further reduce the already low levels of serum ketones and PPARα and Cpt1a mRNAs observed in old animals (Fig. 4a, b). Furthermore, in aged mice, fasting did not inhibit liver mTORC1 activity to nearly the same degree as in young mice (Fig. 4c). Consistent with this defect in mTORC1 inhibition, ageing greatly impaired the fasting-induced exit of NCoR1 from the nucleus and the release of NCoR1 from PPRE-containing promoters

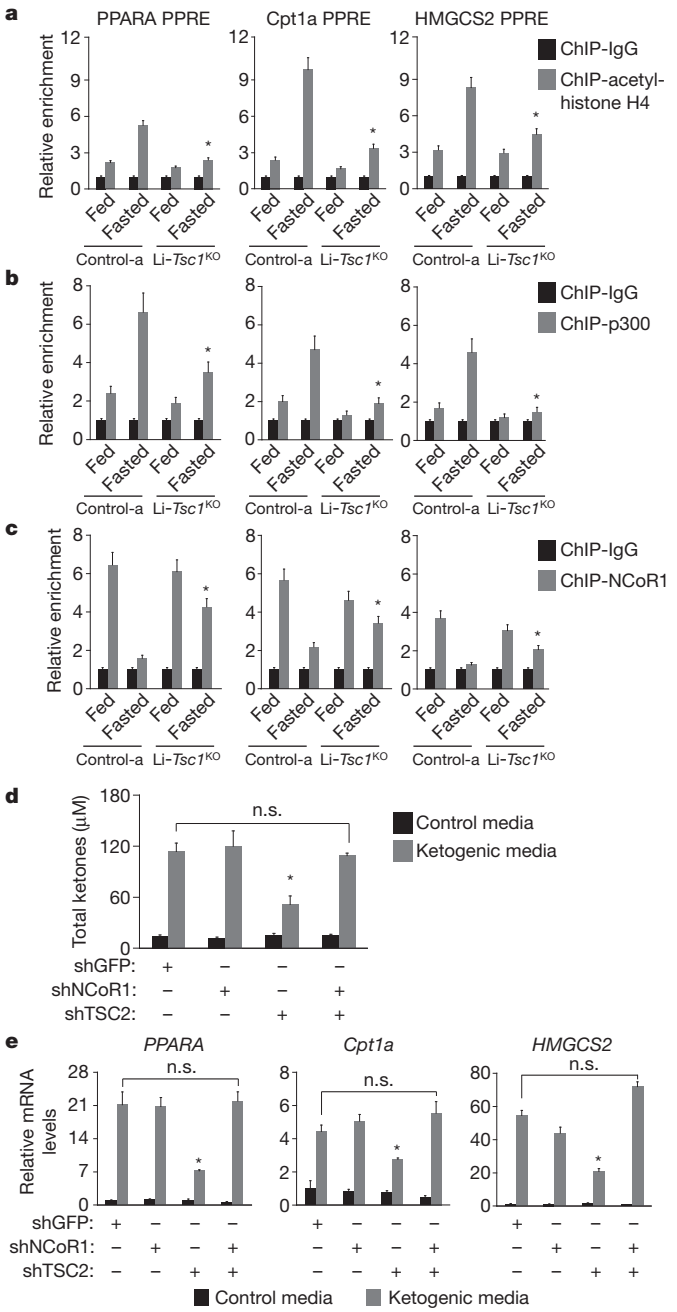


**Figure 3 | mTORC1 requires the NCoR1 corepressor to inhibit PPARα function. a–c**, At PPRE-containing promoters, mTORC1 activation in the liver prevents fasting-induced histone H4 acetylation (**a**), p300 occupancy (**b**), and release of NCoR1 (**c**). Liver extracts from control or Li-*Tsc1*$^{KO}$ mice that were fed or fasted as in Fig. 2a were subjected to ChIP assays (Methods). Values are mean ± s.d. relative enrichment values for $n = 4$. *$P < 0.05$ compared to fasted control mice. **d**, **e**, AML12 cells stably expressing lentiviral shRNAs targeting GFP, NCoR1, TSC2, or NCoR1 and TSC2 were incubated in control or ketogenic media for 3 days and total media ketones (**d**) and indicated mRNA levels were determined as in Fig. 2d (**e**). Values are mean ± s.d. for $n \geq 5$. *$P < 0.05$ compared to shGFP-expressing cells cultured in ketogenic media (**d**, **e**).

(Fig. 4d, Supplementary Fig. 9a). In contrast, in Li-*Rap*$^{KO}$ mice, NCoR1 remained cytoplasmic in the livers of both young and aged animals (Supplementary Figs 8b, 9a). Remarkably, aged Li-*Rap*$^{KO}$ mice did not suffer (unlike aged control mice) a reduction in ketone production or PPARα-target gene expression during fasting (Fig. 4e, f; Supplementary Figs 3d, 9b). Collectively, these findings establish that mTORC1 activity mediates the suppression of hepatic ketogenesis induced by ageing.

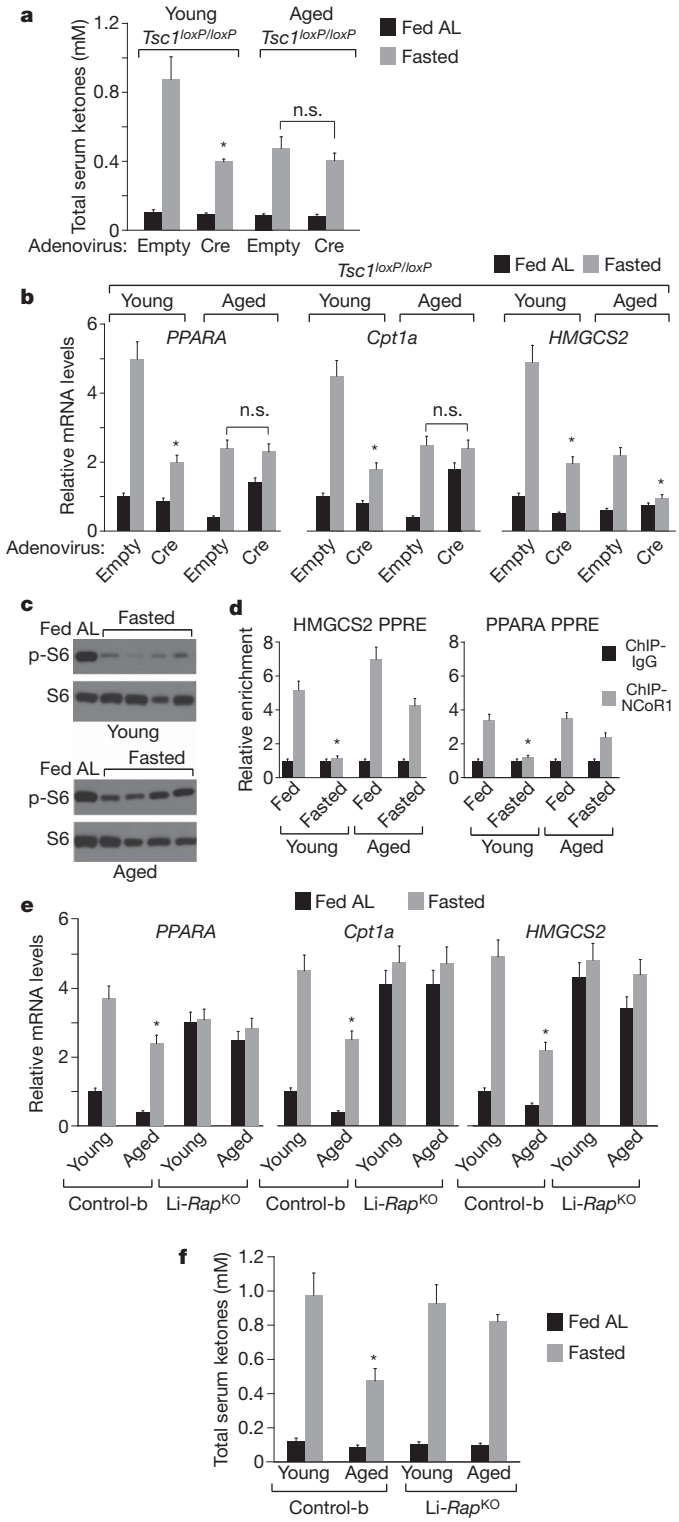


**Figure 4 | mTORC1 mediates the ageing-induced inhibition of PPARα function and ketone production.** **a**, **b**, Young (2–8 months) or aged (20–24 months) mice having the conditional null allele of TSC1 ($Tsc1^{loxP/loxP}$) were injected with an empty adenovirus or a Cre recombinase-expressing adenovirus. Two weeks later, total serum ketones (**a**) and indicated liver mRNA levels (**b**) were measured in fed or fasted mice. Values are mean ± s.d. for $n = 4$. $^*P < 0.05$ compared to fasted young mice administered an empty adenovirus. **c**, Immunoblotting was used to measure the levels of serine 240/244 phosphorylated and total S6 in the livers of fed or fasted control mice that were young or aged. **d**, ChIP assays were performed on indicated liver extracts (Methods). Values are mean ± s.d. for $n = 5$. $^*P < 0.05$ compared to fasted young mice. **e**, **f**, Indicated liver mRNA levels (**e**) and total serum ketones (**f**) were measured in fed or fasted control or Li-$Rap^{KO}$ mice that were young (2–8 months) or aged (20–24 months). Values are mean ± s.d. for $n \geq 5$. $^*P < 0.05$ compared to fasted young control mice.

In conclusion, mTORC1 regulates ketogenesis and PPARα activity in response to fasting and feeding as well as ageing. The control of NCoR1 subcellular localization by mTORC1 may be how mTORC1 regulates PPARα and ketogenesis. Because activated mTORC1 inhibits PPARα function in cells treated with a PPARα agonist, mTORC1 may also regulate PPARα through additional mechanisms, such as by preventing PPARα from responding appropriately to ligand binding or by inhibiting PPARα coactivators. The finding that mTORC1 promotes an ageing phenotype in the liver is consistent with substantial evidence showing that inhibition of the TORC1 pathway elongates lifespan in diverse organisms[16,17]. If mTORC1 regulates PPARα in other organs besides the liver, our findings may be relevant to the ageing-induced decline in PPARα function that is known to occur in organs besides the liver[18].

## METHODS SUMMARY

All animal studies and procedures were approved by the MIT Institutional Animal Care and Use Committee. Mice were given chow *ad libitum*, fasted or refed for the indicated times and indicated serum metabolites were measured. Hepatic metabolite measurements (20), *ex vivo* fatty acid oxidation (19) and ketogenesis assays (19), and sodium octanoate(10), rapamycin (21) and WY 14643 (3) administrations were performed as previously described[3,10,19–21]. Chromatin immunoprecipitation assays were performed using a kit from Millipore according to the manufacturer's instructions. Significance *P* values were obtained by performing non-paired, two-tailed Student's *t*-tests to compare two groups.

**Full Methods** and any associated references are available in the online version of the paper at www.nature.com/nature.

**Received 28 February; accepted 13 October 2010.**


1. Sarbassov, D. D., Ali, S. M. & Sabatini, D. M. Growing roles for the mTOR pathway. *Curr. Opin. Cell Biol.* **17,** 596–603 (2005).
2. Desvergne, B. & Wahli, W. Peroxisome proliferator-activated receptors: nuclear control of metabolism. *Endocr. Rev.* **20,** 649–688 (1999).
3. Dowell, P. *et al.* Identification of nuclear receptor corepressor as a peroxisome proliferator-activated receptor α interacting protein. *J. Biol. Chem.* **274,** 15901–15907 (1999).
4. Sanguino, E. *et al.* Lack of hypotriglyceridemic effect of gemfibrozil as a consequence of age-related changes in rat liver PPARα. *Biochem. Pharmacol.* **67,** 157–166 (2004).
5. Sastre, J. *et al.* Aging of the liver: age-associated mitochondrial damage in intact hepatocytes. *Hepatology* **24,** 1199–1205 (1996).
6. Polak, P. & Hall, M. N. mTOR and the control of whole body metabolism. *Curr. Opin. Cell Biol.* **21,** 209–218 (2009).
7. Huang, J. & Manning, B. D. A complex interplay between Akt, TSC2 and the two mTOR complexes. *Biochem. Soc. Trans.* **37,** 217–222 (2009).
8. Michael, M. D. *et al.* Loss of insulin signaling in hepatocytes leads to severe insulin resistance and progressive hepatic dysfunction. *Mol. Cell* **6,** 87–97 (2000).
9. Gavrilova, O. *et al.* Torpor in mice is induced by both leptin-dependent and -independent mechanisms. *Proc. Natl Acad. Sci. USA* **96,** 14623–14628 (1999).
10. McGarry, J. D. & Foster, D. W. The regulation of ketogenesis from octanoic acid. The role of the tricarboxylic acid cycle and fatty acid synthesis. *J. Biol. Chem.* **246,** 1149–1159 (1971).
11. McGarry, J. D., Meier, J. M. & Foster, D. W. The effects of starvation and refeeding on carbohydrate and lipid metabolism *in vivo* and in the perfused rat liver. The relationship between fatty acid oxidation and esterification in the regulation of ketogenesis. *J. Biol. Chem.* **248,** 270–278 (1973).
12. Hsu, M. H., Savas, U., Griffin, K. J. & Johnson, E. F. Identification of peroxisome proliferator-responsive human genes by elevated expression of the peroxisome proliferator-activated receptor α in HepG2 cells. *J. Biol. Chem.* **276,** 27950–27958 (2001).
13. Hashimoto, T. *et al.* Defect in peroxisome proliferator-activated receptor α-inducible fatty acid oxidation determines the severity of hepatic steatosis in response to fasting. *J. Biol. Chem.* **275,** 28918–28928 (2000).
14. Guan, H. P., Ishizuka, T., Chui, P. C., Lehrke, M. & Lazar, M. A. Corepressors selectively control the transcriptional activity of PPARγ in adipocytes. *Genes Dev.* **19,** 453–461 (2005).
15. Glass, C. K. & Rosenfeld, M. G. The coregulator exchange in transcriptional functions of nuclear receptors. *Genes Dev.* **14,** 121–141 (2000).
16. Stanfel, M. N., Shamieh, L. S., Kaeberlein, M. & Kennedy, B. K. The TOR pathway comes of age. *Biochim. Biophys. Acta* **1790,** 1067–1074 (2009).
17. Harrison, D. E. *et al.* Rapamycin fed late in life extends lifespan in genetically heterogeneous mice. *Nature* **460,** 392–395 (2009).

18. Iemitsu, M. *et al.* Aging-induced decrease in the PPAR-α level in hearts is improved by exercise training. *Am. J. Physiol. Heart Circ. Physiol.* **283,** H1750–H1760 (2002).
19. Faraj, M. & Cianflone, K. Differential regulation of fatty acid trapping in mouse adipose tissue and muscle by ASP. *Am. J. Physiol. Endocrinol. Metab.* **287,** E150–E159 (2004).
20. Folch, J., Lees, M. & Sloane Stanley, G. H. A simple method for the isolation and purification of total lipides from animal tissues. *J. Biol. Chem.* **226,** 497–509 (1957).
21. Cunningham, J. T. *et al.* mTOR controls mitochondrial oxidative function through a YY1-PGC-1α transcriptional complex. *Nature* **450,** 736–740 (2007).

**Supplementary Information** is linked to the online version of the paper at www.nature.com/nature.

**Acknowledgements** We thank S. Biddinger and C.R. Kahn for providing the $Ir^{loxP/loxP}$ and Li-$Ir^{KO}$ mice; D. Kwiatkowski for the $Tsc1^{loxP/loxP}$ mice; R. Zoncu for assistance with imaging experiments and image analysis; F. Reinhardt for assistance in animal virus injections; and T. Jacks, L. Guarente, V. Mootha and members of the Sabatini laboratory for support and discussions. This research was supported by fellowships from the American Diabetes Association and Ludwig Cancer Fund to T.R.P.; a fellowship from the Canadian Institutes of Health Research to M.L.; and NIH grants CA103866 and CA129105 to D.M.S. D.M.S. is an investigator of the Howard Hughes Medical Institute.

**Author Contributions** S.S. and D.M.S. conceived the project and designed the experiments, S.S. performed the experiments, and T.R.P. aided in generating the Li-$Rap^{KO}$ mice and adenovirus preparations. M.L. assisted in metabolite measurements and animal dissections. S.O. assisted with animal dissections and husbandry. S.S. wrote and D.M.S. edited the manuscript.

**Author Information** Reprints and permissions information is available at www.nature.com/reprints. The authors declare no competing financial interests. Readers are welcome to comment on the online version of this article at www.nature.com/nature. Correspondence and requests for materials should be addressed to D.M.S. (sabatini@wi.mit.edu).

## METHODS

**Materials.** TSC1$^{loxP/loxP}$ mice and Li-*Ir*$^{KO}$ mice were gifts from D. Kwiatkowski (Harvard Medical School) and C.R. Kahn (Joslin Diabetes Center), respectively. Antibodies to TSC1, raptor, phospho-S235/236 S6, phospho-240/244 S6, and S6 were purchased from Cell Signaling Technology; the antibody to NCoR1 for ChIP experiments and immunofluorescence assays from Abcam (ab24552); the antibody to NCoR1 for immunofluorescence studies from Thermo Scientific (PA1-844A); the p300 (sc-585x) and PPARα (sc-9000x) antibodies from Santa Cruz Biotechnology; antibodies to the acetyl-histone H4 (06-866) from Millipore; and the Cy3-conjugated secondary antibody from Invitrogen. WY-14643 was purchased from Cayman chemicals; rapamycin from LC Labs; dexamethasone, transferrin, insulin, sodium octanoate, selenium, trichostatin A, and oleic acid from Sigma; radiolabelled oleic acid from Perkin Elmer; PPARα-expressing adenovirus from Vector Biolabs; high-titre empty adenovirus and Cre recombinase-expressing-adenovirus from the Gene Transfer Vector Core at the University of Iowa; and AML12 cells from ATCC. Lentiviral shRNAs targeting murine TSC1, TSC2 and NCoR1 were obtained from The RNAi Consortium (TRC) collection of the Broad Institute[22] and from Sigma-Aldrich. The sequences for each shRNA are as follows. shNCoR1, CCGGCCTCTAATACAGGCACTTCAACTCGAGTTGAAGTGCCTGTATTAGAGGTTTTTG; shTsc1, CCGGGCCAGTGTTTATGCCCTCTTTCTCGAGAAAGAGGGCATAAACACTGGCTTTTTG; shTsc2, CCGGGCCCGATATGTGTTCTCCAATCTCGAGATTGGAGAACACATATCGGGCTTTTTG; shGFP, CCGGTACAACAGCCACAACGTCTATCTCGAGATAGACGTTGTGGCTGTTGTATTTTT.

**Generation of Li-*Tsc1*$^{KO}$ and Li-*Rap*$^{KO}$ mice.** Mice carrying a floxed allele of TSC1 (*Tsc1*$^{loxP/loxP}$)[23] were backcrossed to C57BL/6 mice for three generations, and then bred to homozygosity. For liver-specific recombination of the floxed TSC1 allele, 100 µl of high-titre adenoviral-Cre ($(3–6) \times 10^{10}$ p.f.u. ml$^{-1}$) was administered via retro-orbital injection under isoflurane anaesthesia to mice ranging from 2 to 20 months in age, and subsequent experiments were performed within a month. PCR genotyping for the floxed and recombined allele was performed as previously described[23]. For generation of Li-*Rap*$^{KO}$ mice, a BAC clone (identifier: RP24-125C11, strain: C57BL/6J) containing raptor exon 6 was obtained from the RPCI-24 mouse genomic DNA library[24]. Standard PCR and cloning procedures were used to generate fragments spanning 4.3 kb upstream of raptor exon 6 and 2.6 kb downstream of and including raptor exon 6 (as well as a 3′ LoxP site downstream of raptor exon 6) that were subsequently assembled together into the PGKneoF2L2DTA vector[25]. In the final targeting construct, the neomycin resistance (neo) cassette was flanked by one 5′ LoxP site and 5′ and 3′ Flp recognition target (Frt) recombination sites. Raptor exon 6 was flanked by a 5′ and 3′ LoxP site located 111 bp upstream and 547 bp downstream, respectively. The targeting vector was linearized and electroporated into embryonic stem cells derived from 129/SvEv mice[26]. Clones were analysed for correct integration by Southern blot and PCR analysis. Chimaeric mice were obtained by microinjection of the correctly targeted clones into BALB/C blastocysts and crossed with C57BL/6 mice to obtain offspring with germline transmission. Mice analysed in this study were backcrossed to C57BL/6 for four generations. Some of the backcrosses involved mice constitutively expressing the FLP recombinase so as to excise the neomycin cassette from the targeted allele[27]. Mice were bred to homozygosity for the floxed raptor allele (*Rap*$^{loxP/loxP}$), and then crossed to mice expressing the Cre-recombinase transgene from the liver-specific albumin promoter[28]. PCR genotyping of *Rap*$^{loxP/loxP}$ and Li-*Rap*$^{KO}$ mice was performed with the following primers that detect the following. 3′ LoxP site of targeted raptor allele: forward, CTCAGTAGTGGTATGTGCTCAG; reverse, GGGTACAGTATGTCAGCACAG. This PCR reaction generates an amplicon of 174 bp when the 3′ LoxP site is present and of 140 bp when the wild-type allele is present.

Albumin Cre recombinase: forward, GTTAATGATCTACAGTTATTGG; reverse, CGCATAACCAGTGAAACAGCATTGC. This PCR reaction generates an amplicon of ~500 bp and indicates the presence of the transgene.

In all experiments involving the Li-*Tsc1*$^{KO}$ mice, the control mice were *Tsc1*$^{loxP/loxP}$ mice that were administered 'empty' adenovirus of a similar titre as the Cre-expressing adenovirus (called 'control-a' mice in figures). For all experiments involving Li-*Rap*$^{KO}$ mice, the control mice were *Rap*$^{loxP/loxP}$ mice that did not have the Albumin Cre transgene ('control-b' mice in figures). For the experiment involving Li-*Ir*$^{KO}$ mice, the control mice were *Ir*$^{loxP/loxP}$ mice that did not have the Albumin Cre transgene ('control-c' mice in figures). No significant changes in body weight, adiposity or satiety were observed in Li-*Tsc1*$^{KO}$ and Li-*Rap*$^{KO}$ mice compared to their respective controls. The increased liver size of Li-*Tsc1*$^{KO}$ mice did not affect the sizes of other organs.

**Animal experiments.** WY-14643 was suspended in 10% DMSO, 90% corn oil at 1.5 mg ml$^{-1}$ and was administered via oral gavage to mice for 5 consecutive days at a dose of 25 mg kg$^{-1}$(ref. 29). 500 mM sodium octanoate in 0.9% sodium chloride was given to mice via intra-peritoneal injections at a dose of 6 µl per gram of body weight (ref. 30). Rapamycin was given to mice via intra-peritoneal injections at a dose of 10 mg per kg body weight (ref. 31). For hepatic overexpression of GFP and PPARα, mice were administered high-titre adenovirus expressing either cDNA via retro-orbital injection under isoflurane anaesthesia and killed 5 days later. For depletion of NCoR1 in the liver, mice were administered high-titre adenovirus expressing shRNAs targeted to NCoR1 or lacZ via retro-orbital injection under isoflurane anaesthesia and killed 6 days later. Low titre adenovirus expressing shRNAs were constructed using the Block-iT Adenoviral RNAi Expression System (Invitrogen) per manufacturer's instructions. High-titre virus was generated by infecting HEK-293T cells with low-titre virus ($10^{10}$ p.f.u. ml$^{-1}$), waiting until some cell death was observed, and then concentrating 200 ml of the culture media into 1 ml using the Vivapure AdenoPACK 100 (Sartorius Stedim Biotech). Fasting experiments began at lights out and ended after the times indicated in the figures. Activity measurements were performed in cages where infrared light beams were placed every 1.5 inches along the length of the cage and beam breaks were measured using a digital counter. Body temperature was measured using an anal probe accurate to 0.1 °C. All experiments were carried out with approval from the Committee for Animal Care at MIT and under supervision of the Department of Comparative Medicine at MIT.

**Immunofluorescence assays.** Immunofluorescence-based imaging of NCoR1 was performed as follows: fixed liver tissue was embedded in paraffin and 3–5 µM thick sections placed on microscope slides. Paraffin-coated sections were then de-waxed using EZ-DeWax deparaffinization solution (BioGenex), placed in boiling citrate buffer, pH 6.0 for ten minutes, and then blocked in PBS with 0.1% Tween-20 and 5% goat serum. Sections were stained overnight with the primary antibody in blocking solution at 4 °C, washed 3 times in PBS/Tween and then incubated at room temperature with Cy3-conjugated secondary antibody in blocking solution for 45 min. Sections were incubated in Hoechst solution for 10 min to stain the DNA, and then coverslipped. Immunofluorescence assays in AML12 cells were performed as previously described[32]. Tiled images were obtained from an inverted epifluorescence microscope (Zeiss) and the exposure time for each channel was kept constant for all slides on a given day. Signal intensity was quantified using ImageJ (NIH) as described below. The PA1-844A antibody (Thermo Scientific) was used for the NCoR1 immunofluorescence studies shown in the figures. Equivalent results were also obtained with the ab24552 (Abcam) antibody.

**Image analysis.** Quantification of fluorescence intensity, pixel location, and hepatocyte size were performed using the NIH software ImageJ. Greyscale 1,048 × 792 pixel images acquired at 63× magnification of cells immunostained with the anti-NCoR1 antibody were used for measuring cellular NCoR1 localization. For each condition, 6 cells from 2 individual images from each liver were measured for a total of 12 cells per liver and thus 60 cells per condition. A line 90 pixels in length, which was sufficiently long to span the nucleus and some of the surrounding cytoplasmic area of all cells, was placed over each cell, such that the midpoint of the line was over the centre of the circle defined by the nucleus. The pixel intensity along the line was then recorded. Given the variability in nuclei size, the width of multiple nuclei per experimental group was also measured. A shaded area, whose width equals the mean diameter of the nuclei plus one standard deviation, was then superimposed upon the plots of pixel intensity of the NCoR1 staining to indicate the cellular location of the pixel intensity measurements.

**Serum metabolite and hepatic measurements.** Tail blood or blood obtained from retro-orbital bleeds at the time of death was centrifuged at low speed at 4 °C for 30 min and serum isolated for metabolite measurements. Total ketones were measured using a colorimetric assay from Wako Chemicals according to manufacturer's protocol. Total glucagon levels were measured using an ELISA kit from Wako Chemicals. True serum triglycerides were measured using a kit from Sigma, and values represent total triglycerides minus serum glycerol. Non-esterified free fatty acids were measured with a colorimetric assay from Roche, while serum insulin was measured using an ELISA kit from DSLabs. Serum glucose measurements were taken from tail blood using an instant glucometer (Ascensia Elite). Hepatic triglycerides were extracted as previously described[33], and measured as above.

**Quantitative RT–PCR.** Total RNA was isolated from cells and tissues using the RNeasy kit from Qiagen. Equal amounts of total RNA for each sample was used for oligo-d(T) (Invitrogen) primed reverse transcription into cDNA using SuperScript II (Invitrogen). Primers for real-time PCR were obtained from Integrated DNA Technologies. Reactions were run on an Applied Biosystems Prism machine using Sybr Green Master Mix (Applied Biosystems). The amount of β-actin cDNA was used to normalize results from gene-specific reactions. Primer sequences used to produce gene-specific amplicons are as follows. NCOR1: forward, GAAGCCACAGCAGAAGAACC; reverse, ACGACCATGTTCTACCAGGC. HMGCS2: forward, ATACCACCAACGCCTGTTATGG; reverse: CAATGTCACCACAGACCACCAG. PPARA: forward, AGAGCCCCATCTGTCCTCTC; reverse,

ACTGGTAGTCTGCAAAACCAAA. CPT1a: forward, CCATGAAGCCCTCA AACAGATC; reverse: ATCACACCCACCACCACGATA. TSC1: forward, ATGGCCCAGTTAGCCAACATT; reverse, GCTGAGAATTGGTTTCCAGGT. β-Actin: forward, GGCTGTATTCCCCTCCATCG; reverse: CCAGTTGGTAA CGCCATGT. HMGCL: forward, ACTACCCAGTCCTGACTCCAA; reverse: TAGAGCAGTTCGCGTTCTTCC. PEPCK: forward, CGATGACATCGCCTGG ATGA; reverse, TCTTGCCCTTGTGTTCTGCA. ACOX: forward, GCCTGAG CTTCATGCCCTCA; reverse, ACCAGAGTTGGCCAGACTGC.

***Ex vivo* liver measurements.** The hepatic *ex vivo* fatty-acid oxidation assay was performed as previously described[34]. Briefly, livers were removed from mice and three ~40 mg portions were placed in individual wells of a 24-well plate along with 1 ml of Krebs-Ringer saline and 1 mM $^3$H-oleic acid-BSA (final concentration was 1 μCi per mM $^3$H-oleic acid). Livers were incubated at 37 °C and 5% oxygen for 2 h. After two hours, the medium was removed, 10 μl was retained for ketone measurements, and the rest transferred to an Eppendorf tube with no cap. Tubes were placed in scintillation vials that contained 2 ml of water, wrapped in aluminium foil, and incubated overnight at 65 °C. The next day the vials were cooled at 4 °C for 30 min, the Eppendorf tube was removed, scintillation fluid was added, and the levels of $^3H_2O$ were measured using a scintillation counter.

***In vitro* ketogenesis in AML12 cells.** For passaging, AML12 cells were cultured in medium prescribed by ATCC that contains insulin and serum. For induction of ketogenesis, cells were first grown to confluence, washed once with PBS, and then incubated in media devoid of serum and insulin and containing 50 μM WY-14643 and 2 mM sodium octanoate. At indicated times, aliquots of the media were removed and total ketone levels measured. Total RNA was also isolated from each well and used to normalize media ketone levels between wells. When employed, lentiviral shRNAs were used as described[32]. Using qRT–PCR, all shRNAs were validated to knockdown their respective targets by at least 70% (Supplementary Fig. 2a, b).

**Chromatin immunoprecipitation assays.** Chromatin immunoprecipitation assays were performed using a kit from Millipore according to the manufacturer's instructions. Liver portions were crosslinked in 1.5% formaldehyde in PBS for 15 min at room temperature, and the reaction was quenched with 0.125 M glycine. Liver cells were disaggregated using 20 gauge syringe needles. Resulting cells were then lysed in 1% SDS lysis buffer for 10 min, and sonicated at 30 s intervals for a total of 5 min. Resulting lysates were diluted in buffer containing 0.01% SDS, 1.1% Triton, 1.2 mM EDTA, 167 mM NaCl and 16.7 mM Tris-HCl. Diluted lysates were pre-cleared with protein-A agarose/salmon sperm and then incubated overnight at 4 °C with 3 μl of NCoR1 antibody, 5 μl of acetyl-histone H4 antibody, and 4 μg of p300 antibody or 4 μg IgG per $10^6$ cells. The next day, the antibodies were captured with protein-A agarose/salmon sperm for 1 h, pelleted, and subjected to washes in low salt, high salt, LiCl and TE buffers contained in the Millipore kit. The chromatin was eluted from antibodies with 1% SDS and 0.1 M $NaHCO_3$, and the crosslinks reversed by heating at 65 °C for 4 h. The chromatin was treated with proteinase K, purified using the High Pure PCR Template Preparation Kit from Roche, and used for PCR analysis. AML12 cells were processed with the same protocol except beginning at the step in which cells are lysed in 1% SDS lysis buffer. The primers below were used to amplify a 150–200 bp amplicon encompassing the PPRE of the indicated genes. As both a negative control and to ensure that proper shearing length was achieved for genomic DNA, PCR was also performed for an amplicon within the second intron of Cpt1a. PPARA PPRE: forward, TTCCGAACCATTCTTTCCAG; reverse, GCTGCCTTCTTTTGCAGAGT. HMGCS2 PPRE: forward, TGAGCCACTCAGCAGAGGAATCAG; reverse: CTGGGTTGGGCTTTATAAGACTCC. CPT1a PPRE: forward, CTTTCCTA CTGAGGCCCAGATAG; reverse: TACAGCCTAGAACCCTGACTGC. CPT1a Intron: forward, CTGGTTGGAATAGGTGTGTCACTG; reverse, ATTGGGGC TGGCTTACAGGTTC.


22. Moffat, J. *et al.* A lentiviral RNAi library for human and mouse genes applied to an arrayed viral high-content screen. *Cell* **124,** 1283–1298 (2006).
23. Uhlmann, E. J. *et al.* Astrocyte-specific TSC1 conditional knockout mice exhibit abnormal neuronal organization and seizures. *Ann. Neurol.* **52,** 285–296 (2002).
24. Osoegawa, K. *et al.* Bacterial artificial chromosome libraries for mouse sequencing and functional analysis. *Genome Res.* **10,** 116–128 (2000).
25. Hoch, R. V. & Soriano, P. Context-specific requirements for Fgfr1 signaling through Frs2 and Frs3 during mouse development. *Development* **133,** 663–673 (2006).
26. Nagy, A., Rossant, J., Nagy, R., Abramow-Newerly, W. & Roder, J. C. Derivation of completely cell culture-derived mice from early-passage embryonic stem cells. *Proc. Natl Acad. Sci. USA* **90,** 8424–8428 (1993).
27. Rodríguez, C. I. *et al.* High-efficiency deleter mice show that FLPe is an alternative to Cre-loxP. *Nature Genet.* **25,** 139–140 (2000).
28. Postic, C. & Magnuson, M. A. DNA excision in liver by an albumin-Cre transgene occurs progressively with age. *Genesis* **26,** 149–150 (2000).
29. Issemann, I. & Green, S. Activation of a member of the steroid hormone receptor superfamily by peroxisome proliferators. *Nature* **347,** 645–650 (1990).
30. McGarry, J. D. & Foster, D. W. The regulation of ketogenesis from octanoic acid. The role of the tricarboxylic acid cycle and fatty acid synthesis. *J. Biol. Chem.* **246,** 1149–1159 (1971).
31. Cunningham, J. T. *et al.* mTOR controls mitochondrial oxidative function through a YY1-PGC-1α transcriptional complex. *Nature* **450,** 736–740 (2007).
32. Sancak, Y. *et al.* The Rag GTPases bind raptor and mediate amino acid signaling to mTORC1. *Science* **320,** 1496–1501 (2008).
33. Folch, J., Lees, M. & Sloane Stanley, G. H. A simple method for the isolation and purification of total lipides from animal tissues. *J. Biol. Chem.* **226,** 497–509 (1957).
34. Faraj, M. & Cianflone, K. Differential regulation of fatty acid trapping in mouse adipose tissue and muscle by ASP. *Am. J. Physiol. Endocrinol. Metab.* **287,** E150–E159 (2004).